Integrated Demand Side Management and Generation Control for Frequency Control of a Microgrid using PSO and FA based Controller

Abdul Latif*‡, D C Das*, S. Ranjan*, I. Hussain*

*Department of Electrical Engineering, National Institute of Technology, Silchar, India, 788010

(latif1014@gmail.com, dulal_nit@yahoo.co.in, ranjan4c@gmail.com, israfilhussain1@gmail.com)

‡ Corresponding Author; Abdul Latif, Department of Electrical Engineering, National Institute of Technology, Silchar, India, 788010, Tel: +91 3842 242912, Fax: +91 3842 242912, latif1014@gmail.com

Received: 24.10.2017 Accepted:24.12.2017

Abstract- This paper investigates demand side management (DSM) method as a new control strategy for frequency control of a microgrid powered by diesel driven generator (DDG), wind and solar photovoltaic (PV) power sources in absence of battery energy storage. Frequency fluctuation due to intermittent power generation is leveled by adjusting the power consumption of the non-critical loads (i.e., heat pump, freezer) and charging-discharging of plug-in hybrid vehicles (PHEV) through the demand response controllers beside the automatic generation control of DDG. The parameters of the controllers (PI/PID) are optimized using popular Particle Swarm Optimization (PSO) and Firefly Algorithm (FA). Different disturbance conditions such as step perturbation and random variations of load, solar PV and wind output power are considered to investigate the performance of the microgrid. Simulation studies confirmed that the performance of the FA optimized PID controller is the best among all other the controllers considered in this study in terms of frequency deviation and setting time.

Keywords: Demand side management (DSM), Demand Response Controller (DR controller), Direct load control (DLC), Plug-in hybrid electric vehicle (PHEV), Heat Pump (HP), Freezer (FREEZER), Microgrid, Frequency deviation.

Nomenclature

Δf	System frequency deviation.
K_{sys}	Frequency characteristics constant of micro-grid.
$G_{sys}(s)$	Transfer function of hybrid micro-grid.
P_{PV}, P_{WTG} and P_{DDG}	Output power of solar PV, wind turbine generator and diesel driven generator, respectively.
$G_{PV}(s)$, $G_{DDG}(s)$, $G_{PHEV}(s)$ $G_{HP}(s)$, $G_{FREEZER}(s)$ and $G_{WTG}(s)$	Transfer function of solar PV system, diesel driven generator, plug-in hybrid electric vehicle, heat pump, freezer and wind turbine generator, respectively.
T_{DDG}, K_{DDG}	Time constant and gain of diesel driven generator.
P_{PHEV}	Power absorbed (or supplied) by plug-in hybrid electric vehicle.
T_{PHEV}, K_{PHEV}	Time constant and gain of plug-in hybrid electric vehicle.
P_{HP}, $P_{FREEZER}$	Power of consumed by Heat pump and Freezer, respectively.
T_{HP} , K_{HP}	Time constant and gain of heat pump.
$T_{FREEZER}$, $K_{FREEZER}$	Time constant and gain of freezer.
P_S	Total power generation of the system.
P_{LOAD}	Power absorbed by the critical load.
ΔP_e	Error in power supply and demand.
M, D	Inertia constant and damping constant of hybrid micro-grid.
R	Droop of the diesel driven generator.
T_{PV}, K_{PV}	Time constant and gain of solar PV system.
T_{WTG}, K_{WTG}	Time constant and gain of wind turbine generator.
W^{max}, W^{min}	Maximum and minimum weight factor for PSO.
C_1 , C_2	Cognitive and social acceleration factors.

1. Introduction

The modus operandi of conventional (fossil fuels-based) power generation system is agreed to be non-optimum and unsustainable in its long run process. So, electricity generations are facing fundamental changes in upcoming decades across the world, due to future grid requires low carbon emissions from generation with higher integration of clean energy resources such as solar, wind, tidal, biomass etc. [1]. Renewable based integrated hybrid power system in the form of standalone or isolated micro grid is believe to be the better choice than conventional centralized power plants due to its small scale, on-site distributed energy, economic reason and energy security [2]. However, characteristics of renewable sources such as volatility, stochasticity and intermittency make it difficult to control the power output of these resources, thus maintaining power balance between supply and demand becomes challenging task. The imbalance between demand and generation causes frequency fluctuation that leads the network towards undesirable situation like system instability, load shedding which are badly effecting the quality of power supply. When demand exceeds the available supply, the frequency falls below 50Hz (or 60 Hz in North America), similarly the reverse case occurs [3]. Unlike the conventional grid, frequency regulation in the isolated microgrid become exacting task due to inclusion of intermittent renewable energy resources (RERs) which are uncontrollable in nature, smaller in size and has less inertia. Therefore, an appropriate control strategy needs to be employed with such a microgrid [4].

Frequency control of renewable energy based hybrid power systems using different types of controllers have been investigated in the past. Conventional PI controller [5], Fuzzy PID controller [6], PSO based fuzzy controller [7], GA and PSO optimized PI/PID controllers [8] have performed satisfactory to reduce the frequency fluctuation in such hybrid power systems. Noticeably in many of the above mentioned hybrid power systems and [9], [10], [11], [12] battery energy storage has been used to level the power fluctuation. Nonetheless, battery storage systems have some limitations, for instance, battery banks are expensive, require frequent maintenance and disposal of battery is big concern [13]. Thus, finding a feasible solution with minimum storage cost, reduced maintenance, and preserving the environment is a current research demand.

Demand side management (DSM) can be a potential solution to the above frequency control related problem in microgrid. Switching on and off of demand side devices with lesser energy consumption cost presented by Ozturk et al. [14]. However, the localized decision making creates customer discomfort due to curtailment of large number of loads.

Recently, some very good works on demand response frequency control of power system have been reported in [15]. Bao, Yu-Qing, et al. [15] considered demand response control scheme for frequency (decreasing cases) control of power system consisting of single generator and demand response appliances. The parameters of the demand response controller (PI) are optimized using GA. However, to ensure the robustness of the proposed control strategy, performance of the proposed demand response control strategy could be explored considering other uncertainties also. In other work [16], demand response for frequency control of diesel generator, solar PV, fuel cell and based hybrid microgrid in absence of storage has been investigated. To maintain the power balance between generation and demand the output of the soar PV system is adjusted in coordination with diesel generating unit and fuel cell outputs along with demand response control. The performance of the control approach has been assessed considering step changes in load /and or generation. However, in order to examine the effect of practically variable nature of generation and / or load demand on dynamic performance of the microgrid, the performance could be evaluated considering randomly variable characteristics. Not much literature or few have investigated the coordinated control of different generating units incorporating DSM in an autonomous storage free microgrid.

In view of this, present paper explores an automatic coordinated control scheme through DSM for containing frequency of a microgrid without energy storage. The micro grid comprises of wind-turbine generator, solar PV generation, diesel-engine driven generator (DDG), plug-in hybrid electric vehicles (PHEV), heat pump (HP), freezers (FREEZER) as non-critical load and certain critical load. The proposed control strategy combines the direct load control (DLC) under demand side management for non-critical load in addition to automatic generation control (AGC). For direct load control the controllable loads are equipped with controller, called DR controller. Combined operation of both the DR controller and AGC controller maintain the frequency within its' permissible limit.

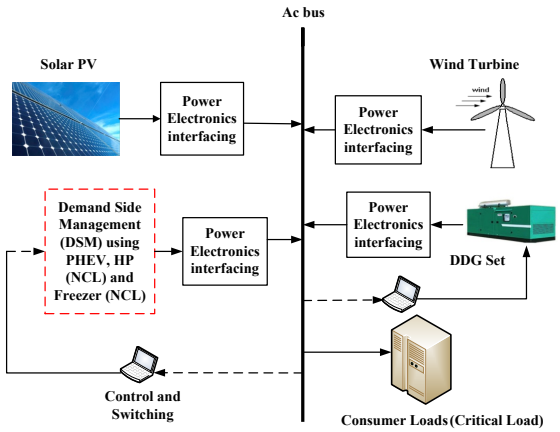

Fig. 1. Conceptual structure of proposed storage free Wind-PV-DDG based microgrid

The objectives of the work are summarized below:

(i) To develop appropriate transfer function model of the proposed microgrid including DLC for controllable loads in MATLAB Simulation software for examining the dynamic performance.
(ii) To optimize the gains of the controllers (PI and PID) employed with DDG for automatic generation control and DR controller for controllable loads using PSO and FA.
(iii) To compare the performance of the controllers (PI and PID) under different operational cases such as step and

random variation in critical load as well as wind and solar power.

(iv) To compare the dynamic performance of the microgrid with DR controllers vis-à-vis its performance without DR controllers.

The rest paper is organized as follows: section 2 explains the complete transfer function of proposed microgrid system. The proposed DSM control philosophy is discussed in section 3. The overview of PSO and FA optimized systems are illustrated in section 4. Problem formulation and Simulation results are presented in section 5 and 6. Consequently, section 7 concludes the findings of the study.

2. Proposed Storage Free Microgrid and Its Modeling

The proposed microgrid along with it's transfer function model are illustrated in Fig. 1 and Fig. 2 respectively. It consists of wind, PV and diesel-based generators along with critical and non-critical loads (i.e., heat pump, freezer). The system parameters shown in appendix, we referred [5, 9, 17,]. The power generated i.e. sum of the output powers from conventional and non-conventional energy resources, are supplied to the critical and non-critical load. The plug-in hybrid electric vehicles supplies power during deficit and draw power when the load exceeds generation. However, heat pump only draws power when load exceeds the generation. The freezer, which is used as a controllable load, capable of reducing the power consumption without causing much discomfort to the consumers during insufficient generation. Modeling, functionalities of each system components and their first order transfer function are discussed in the succeeding sections.

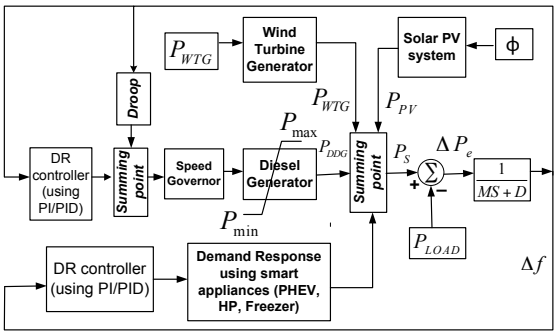

Fig. 2. Schematic transfer function model of proposed microgrid without storage

2.1. Wind turbine generator (WTG) system

Wind energy is considered one of the most rapidly developing renewable energy with an average growth of 21% during the past decades [18]. Wind power is extracted from the kinetic energy of the moving air. Therefore, power generated from the wind turbine generator system is the function of the instantaneous wind speed, V_W. V_W is given by [9],

$$V_W = V_{WB} + V_{WS} + V_{WR} + V_{WN} \tag{1}$$

where V_{WB}, V_{WS}, V_{WR} and V_{WN} are the base wind speed, squall wind speed, speed of ramp wind and speed of noise wind. The mechanical output power of the wind turbine is defined by the following equation [19]:

$$P_m = \frac{1}{2}\rho A C_P(\lambda,\beta)\,V_W{}^3 \tag{2}$$

where ρ represent the air density, A is the swept area of the wind blade, V_W is the wind velocity and C_P (λ,β) is the power conversion coefficient of the wind turbine depending on the tip-speed ratio λ and pitch angle β of the blades. The wind turbine is a nonlinear system and its pitch controller uses to counter act frequency oscillations of the utility grid. Hence the pitch system which controls the pitch angle according to wind speed introduces nonlinearities in the system. The transfer function model depicting first order of wind turbine generator (WTG) [9] is given by

$$G_{WTG}(s) = \frac{K_{WTG}}{1+sT_{WTG}} \tag{3}$$

2.2. Solar PV system

Solar PV system is another fasted growing renewable energy technology. Solar radiation which is intermittent in nature because of dependency on weather condition is used solar photovoltaic cells for electricity generation. The d.c. power so generated is converted to a.c through the inverter. The series/parallel combination of PV solar cells form PV arrays, output power (in watts) of which is given by [9],

$$P_{PV} = \eta S \Phi\{1 - 0.005(T_a + 25)\} \tag{4}$$

where η is the conversion efficiency of PV cell (9% -12%), S is (=4084 m^2) the measured area of PV array, ϕ (=1kW/m^2) is the solar radiation and T_a is ambient temperature in degree Celsius. The d.c. power output of PV generator is given by [16],

$$P_{PV} = V_{dc} * I_{PV} \tag{5}$$

where V_{dc} and I_{PV} is the PV module operating voltage or dc-link voltage and module current respectively. In addition $\Delta P_{PV} = P_{PV\_rated} - P_{PV}$. The transfer function of the PV system can be represented [9] as:

$$G_{PV}(s) = \frac{K_{PV}}{1+sT_{PV}} \tag{6}$$

2.3. Diesel engine driven generator (DDG) system

Diesel engine coupled with synchronous generator produces the required torque for driving the synchronous generator to produce sufficient amount of power output. It acts as a back-up generating unit to maintain load demand during unavailability of solar and/or wind power. In a microgrid sudden changes in load at the customer end occur frequently, so, it is important that prime mover in the diesel generator is efficient enough in addition to fast dynamic response. The energy generated by DDG is given by [20],

$$E_{DDG} = \eta_{DDG} t \int P_{DDG}.dt \tag{7}$$

Where P_{DDG} is the rated output power of DDG and η_{DDG} is its

efficiency and t is the operating time. A diesel engine driven generator is a nonlinear system with time varying dead time between the injection and the production of the mechanical torque [9]. The governor adjusts the fuel injection to the engine through so as to generate required power to maintain the balance between the generation and demand [16]. This work considers first order transfer function model for diesel generator [5].

$$G_{DDG}(s) = \frac{K_{DDG}}{1 + sT_{DDG}} \tag{8}$$

2.4. Plug-in hybrid electric vehicle (PHEV) system

The Plug-in hybrid electric vehicle (PHEV) is a kind of vehicle which can be powered from conventional fuel as well as battery/super capacitor [21]. The PHEV is used to take power from the grid and store it during off-peak hours and supply the store power to the grid during peak hours. The PHEV model is shown in Fig. 3(a). Since it can be run using either fuel or electricity, it is a good option for driving long distance. The transfer function of PHEV represented as 1st order by [5]

$$G_{PHEV}(s) = \frac{K_{PHEV}}{1 + sT_{PHEV}} \tag{9}$$

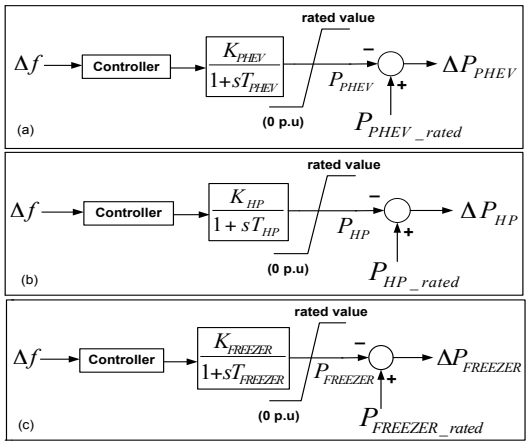

Fig. 3. Shows the model of (a) PHEV (b) HP and (c) Freezer

2.5. Heat pump (HP) system

As the name suggests, the heat pump (HP) is a device used to transfer generated heat through a compressor which pumps the heat mixed with a substance called refrigerant. The refrigerant passes through the heat exchanger coils where the heat is absorbed by the surrounding and the refrigerants get evaporated due to low pressure. There are upward trends to install heat pump in as isolated grid as a controllable load. So, a large scale regulating capacity (by large amount of power consumption) of power fluctuation compensation can be controlled through heat [22]. The HP is modeled as a first order system as shown in Fig. 3(b). The transfer function of HP represented as 1st order by [5]

$$G_{HP}(s) = \frac{K_{HP}}{1 + sT_{HP}} \tag{10}$$

2.6. Freezer system

The family-friendly controllable load freezers have attracted research attention because of their rapid disconnection and storage capability [23]. In freezer dynamic demand control can be used for the frequency response to improve system stability. The system model has been shown in Fig. 3(c). When generation is more, the freezers are switched on so that they can absorb power and when generation falls suddenly the freezer are switched off to maintain frequency. The transfer function of freezer is given by [17]

$$G_{FREEZER}(s) = \frac{K_{FREEZER}}{1 + sT_{FREEZER}} \tag{11}$$

2.7. Power deviation and system frequency deviations

When the system suffers from any disturbance the total power (active power) imbalance, $\Delta P_{e,}$ primarily affects the system frequency. In a wind, solar based microgrid, maintaining system frequency is a tough job. For stable operation of the microgrid, an appropriate control strategy is adopted which effectively maintain the active power balance by adjusting the output of the generating components and controllable loads. As frequency fluctuation occurs mainly due to active power mismatch; the main aim is to keep balance of active power generation and demand. The mismatch between power generation (P_S) and load demand (P_{LOAD}) reference is given by

$$\Delta P_e = P_S - P_{LOAD} \tag{12}$$

Though system frequency is varies with net power variation, the system frequency deviation Δf calculated by [8]

$$\Delta f = \frac{\Delta P_e}{K_{sys}} \tag{13}$$

In practical scenario, there exist an intrinsic time delay between the power deviation and system frequency fluctuation. Thus, the transfer function model of power system for system frequency fluctuation to per unit active power deviation is expressed by [24]

$$G_{sys}(s) = \frac{\Delta f}{[P_S - P_{LOAD}]} = \frac{1}{K_{sys}(1 + sT_{sys})} = \frac{1}{Ms + D} \tag{14}$$

3. Proposed DSM Control Strategy

DSM concept includes preservation of energy and energy efficiency, demand response, fuel replacement, and residential or commercial load management programs [4]. The primary objective of DSM is to shape the consumer needs for energy according to the generation of energy and distribution capacity. Usually when generation is less than demand, loads are curtailed to maintain the system but the main motive of DSM is to encourage the consumers to use less energy during peak hours or to move the time of energy use to the off-peak hour's viz. night.

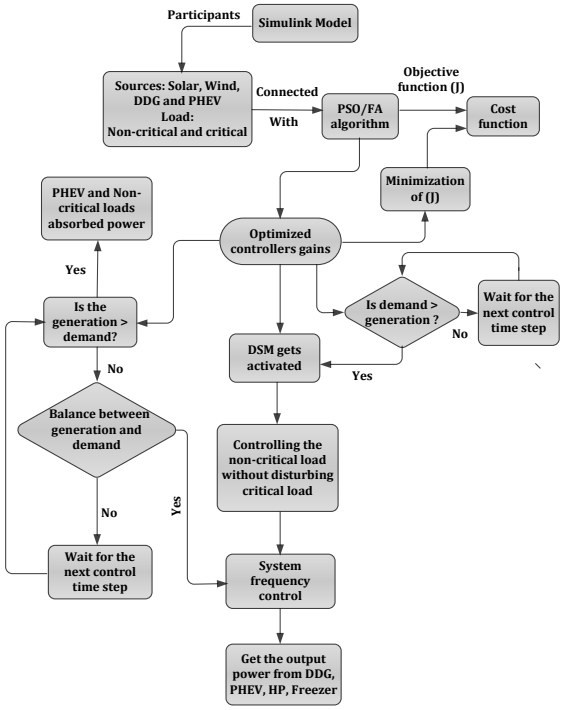

Fig. 4. Flowchart representation of proposed DSM control strategy

In this paper, direct load control (DLC) approach under demand response has been considered to reduce the frequency fluctuation due to variation in load and /or generation from renewable energy. Beside the automatic generation control, AGC (only for DDG), DLC adjust the power consumption by the controllable appliances such as HP, FREEZER and PHEV during frequency fluctuation. Switching off these devices for some time do not cause much inconvenience to the customers. The parameters of the controllers equipped with DDG for AGC as well as the demand response controllers employed with HP, PHEV and FREEZER are optimized using popular soft computing tools such as PSO and FA. The proposed control strategy is expected to be effective in maintaining the system frequency of the microgrid under different uncertainty conditions in absence of battery energy storage.

Since, wind and solar PV are intermittent in nature; the highest capacity non-renewable energy based generator (DDG) should be able to meet the critical load demand. A range of frequency along with upper and lower threshold frequency should be determined above and below which the non-critical loads would be off for maintaining the frequency within the permissible range. The flowchart representation of the proposed DSM control strategy is shown in Fig. 4.

When $P_{PV} + P_{WTG} + P_{DDG} < P_{CL} + P_{NCL}$; DSM control method is activated and controlling the non-critical loads such as heat pump and freezer while keeping the critical load undisturbed. The stored energy in PHEV is fed back to the grid, but when $P_{PV} + P_{WTG} + P_{DDG} > P_{CL} + P_{NCL}$; DSM strategy is off and the non-critical loads are connected in the system, PHEV are charged. Due to the nonlinearities present in the power system, the controller tuning is very difficult task. So the controller's (PI/PID) parameters of the proposed model have been optimized by using Particle Swarm (PSO) Optimization and firefly (FA) algorithms due to their advantage over other techniques.

4. Overview of PSO and FA Algorithm

Russell Eberhart and James Kennedy has developed Particle Swarm Optimization (PSO) algorithm in the year of 1995, which is population-based stochastic optimization technique that is derived from the social-psychological theory and has been found to provide optimal solution in complex system. This technique has been inspired by social behavior of bird flocking, fish schooling and swarm theory [8]. In the past few years, number of paper has been published based on application of PSO. Reference [25] gives a comprehensive overview of PSO and its application in power system. . The flowchart of the PSO algorithm is illustrated in Fig. 5. The PSO optimization mainly has three steps until the satisfactory results are not met.

- Find the fitness function of every particle.
- Compare the fitness value of every individual particle with its best position for particle (Pbest). The best fitness value among all the Pbests is the best global position (gbest).
- Update the velocity and position of every particle. During each iteration, every particle in the swarm is updated by [26] using (15-16).

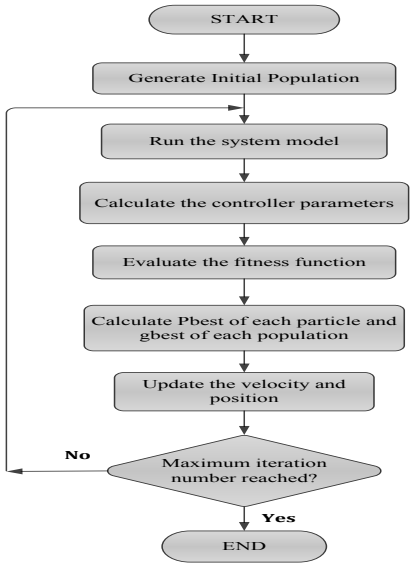

Fig. 5. Flowchart of PSO algorithm

$$v_{i+1} = w.v_i + c_1.rand_1.(\text{pbest} - x_i) + c_2.rand_2.(gbest\text{-}x_i) \quad (15)$$

$$x_{i+1} = x_i + v_{i+1} \quad (16)$$

$$w = w_{\max} - \frac{w_{\max} - w_{\min}}{iter_{\max}} iter \quad (17)$$

where, c_1 and c_2 are the cognitive and social acceleration factors respectively. $rand_1$ and $rand_2$ are the random numbers of range (0,1). w is the inertia weight factor. $iter$ and $iter_{max}$ are the iteration count and maximum iteration respectively.

On the other hand, firefly (FA) algorithm was formulated by X.-S. Yang in 2007 mimicked the flashing characteristics of fireflies. Recently, it has been reported that the FA outperforms the GA in terms of efficiency in finding the global optimum and success rate. The flowchart of the FA algorithm is shown in Fig. 6. The algorithm was developed with the assumption that:

- All fireflies are unisex so that one firefly will be attracting to other fireflies irrespective of their sex.
- Attractiveness is proportional to the brightness, thus for any two flashing fireflies, the less bright one will move towards the bright one. Attractiveness decrease with increase in distance between them. If there is no brighter one then a particular firefly, it will move randomly.
- The brightness of the firefly is determined by the landscape of the objective function. For a maximization problem, the brightness can simply be proportional to the value of objective function. [27, 28]

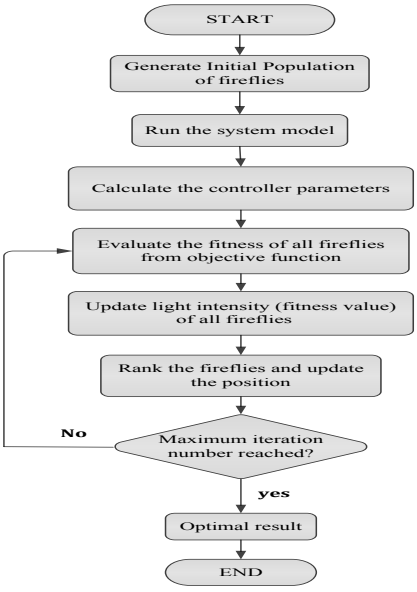

Fig. 6. Flowchart of firefly (FA) algorithm

The distance between two fireflies i and j at X_i and X_j can be the Cartesian distance r_{ij}-X_i-X_j. In the simplest form, the light intensity I(r) varies with the distance monotonically and exponentially. [29]

$$I = I_0 e^{\gamma r} \tag{18}$$

where I, I_0 and γ are the light intensity, the original light intensity and the absorption coefficient. As a firefly's attractiveness is proportional to the light intensity seen by adjacent fireflies, so the attractiveness can be defines as

$$\beta = \beta_0 e^{-\gamma r^2} \tag{19}$$

The exponent γr can be replace by other functions such as γr^m when m > 0 [29]. For more details and pseudo code of FA authors may refer to [29].

The performances of the optimization algorithms are sensitive to their adjusting parameters. The tuned values of parameters of PSO and FA are presented in Table 1.

Table 1. Tuned parameters of PSO and FA

PSO parameters	Value	FA parameters	Value
Number of iteration	200	Number of iteration	200
Population	50	Light absorption coefficient	0.5
W^{max}	0.9	Attractiveness coefficient	0.2
W^{min}	0.1	Number of firefly	50
C_1	2	Scaling factor	0.2
C_2	2	-	-

5. Problem Formulation

The parameters of the (PI/PID) controllers employed with the microgrid are optimized so as to minimize the objective function. The integral square error (ISE) of frequency deviation is chosen as the objective function (J), it is expressed as follows:

$$J = \int_0^{\alpha} (\Delta f)^2 dt \tag{20}$$

The objective is to minimize J, subject to the constraints given below

$$K_{p\_DDG}^{\min} \le K_{p\_DDG} \le K_{p\_DDG}^{\max} \tag{21}$$

$$K_{i\_DDG}^{\min} \le K_{i\_DDG} \le K_{i\_DDG}^{\max} \tag{22}$$

$$K_{d\_DDG}^{\min} \le K_{d\_DDG} \le K_{d\_DDG}^{\max} \tag{23}$$

Similarly, the ranges for the parameters of the other controllers employed with PHEV, HP and FREEZER respectively are chosen. The maximum and minimum values of K_p, K_i and K_d of the each of the controller are taken in the range of [-400 to 400].

6. Simulation Results and Discussion

In this section, the dynamic performance of the proposed DDG-Wind-PV-PHEV based microgrid along with DSM control strategy is evaluated under different power generation and loading condition to ascertain its performance. As the proposed microgrid consists of renewable energies (solar and wind), causes considerable effects on the system frequency. So the system employed with the controllers which regulate the power output from the DDG, PHEV, HP and FREEZER. In order to access the effectiveness of the proposed methodology, the microgrid system under various operating points and disturbance condition with optimum gain setting of PSO and FA based PI and PID controllers respectively, has been simulated. The simulation time of the present system is considered as 100 s. The following four cases are illustrated in Table 2. are considered for case studies.

Table 2. Simulation condition for each case

Case	Operating conditions	DSM activity
Case1	P_{WTG} = 0.3 p.u at 0<t<60s & 0.4 p.u at t>60s, P_{PV} = 0.2 p.u at 0<t <80s & 0.3 p.u at t>80s and P_{CL}=0.5 p.u	During 60<t< 100s PHEV and Non-critical loads absorbed Power.
Case2	P_{WTG} =0.3 p.u at0<t<60s & 0.1p.u at t>60s, P_{PV} = 0.2 p.u at 0<t <80s & 0.1 p.u at t>80s and P_{CL} =0.5 p.u at 0<t<60s.	During 0<t<100 s Non-critical loads are off and at 60<t<100 s PHEV delivers its power.
Case3	P_{WTG} = 0.3 p.u at0<t<60s & 0.4p.u at t>60s, P_{PV} = 0.2 p.u at 0<t <80s & 0.3 p.u at t>80s and P_{CL} = 0.5 p.u at0<t<60s = 0.7 p.u at t>60s.	During 60<t<80 s PHEV delivers its power and Non-critical loads are off.
Case4	P_{WTG}, P_{PV} and P_{CL} are Randomly variable in nature.	During 0<t<100 s, non-critical loads are off and PHEV is variable with random load.

6.1 Step increase in wind and PV power and constant demand condition: Case 1

In this case, the dynamic performance of proposed microgrid is investigated under step disturbance in P_{PV} and P_{WTG}. Fig. 7 represents the P_{WTG}, P_{PV} and load demand (P_{CL}) respectively. The total power generation (P_S) and load (P_{LOAD}) is given by

$$P_S = P_{WTG} + P_{PV} + P_{DDG} \pm P_{PHEV} \quad (24)$$

$$P_{LOAD} = P_{CL} + P_{NCL} \quad (25)$$

Where, P_{CL} and P_{NCL} are the critical load power and non-critical load power. As it can be seen that during 0<t<100s critical load demand is kept constant 50% (.5 p.u) of the nominal value. At t=60s, the wind power output (P_{WTG}) is increase to 0.4 p.u from its initial value of 0.3 p.u and at t=80s, the solar PV power (P_{PV}) is increase to 0.3 p.u from its initial value of 0.2 p.u. During the time period from 0<t<60 s, the total generated power (P_S) is same as load demand (P_{LOAD}), hence there is no power generation by the DDG, PHEV and no need to activate DSM strategy. For the remaining time period DSM strategy works. As there is a surplus power, the HP, FREEZER and PHEV absorb the same.

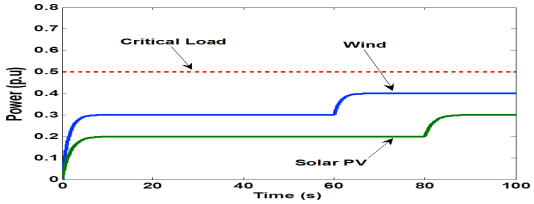

Fig. 7. Output power of P_{WTG}, P_{PV} and load model, case 1

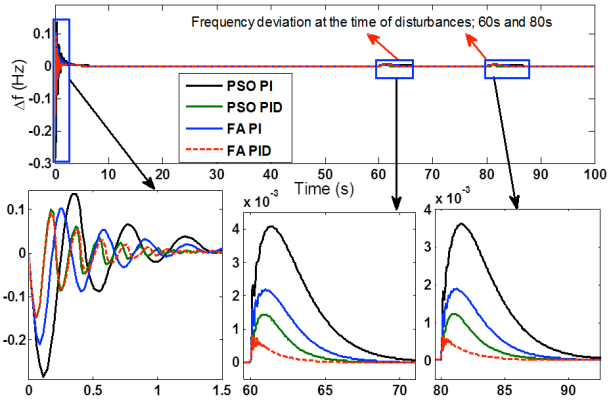

Fig. 8. Frequency deviation Δf observed with PSO and FA optimized PI and PID controllers, case 1

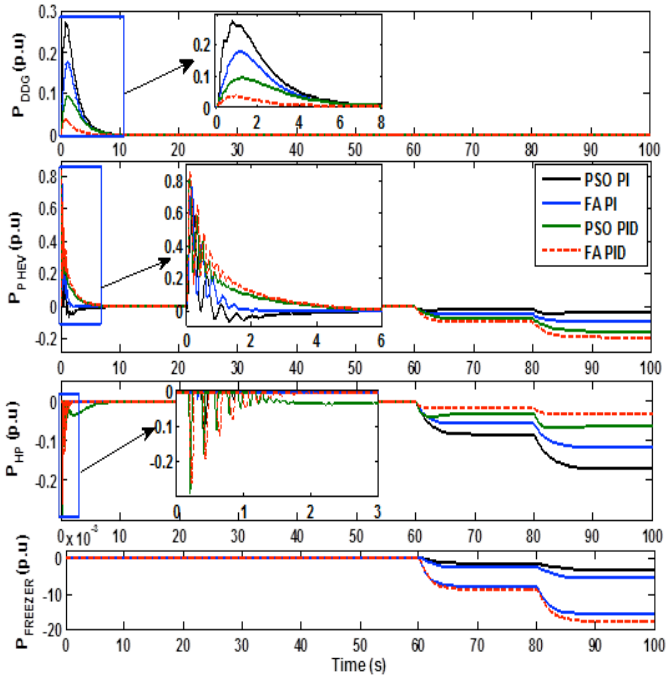

Fig. 9. Output power generation of DDG, PHEV, HP and FREEZER, case 1

Thus, the mismatch between active power generation and consumption of the system is automatically alleviated by the controller to regulate the power variation from DDG, PHEV and non-critical loads which lead to system frequency within its permissible limit. The gains of the controllers are optimized by using PSO and FA are presented in Table 3. and Table 4. respectively. Fig. 8 illustrate the frequency deviation of hybrid power system using PSO and FA optimized PI and PID controllers. The output power from DDG, PHEV, HP and FREEZER are shown in Fig. 9. The convergence plots of the objective function vs iteration for the system using PSO and FA optimized PI/PID controllers are presented in Fig. 10. Frequency deviation and objective function plot reveals that the FA optimized controllers performs betters than their PSO optimized counter part.

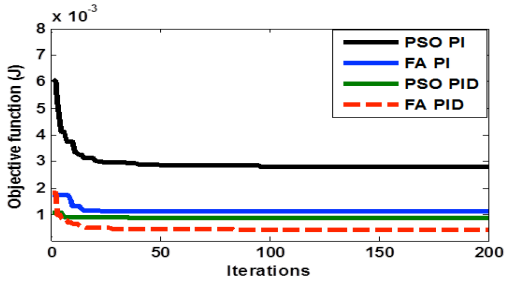

Fig. 10. Objective function vs iteration for PI and PID controller based model, case 1

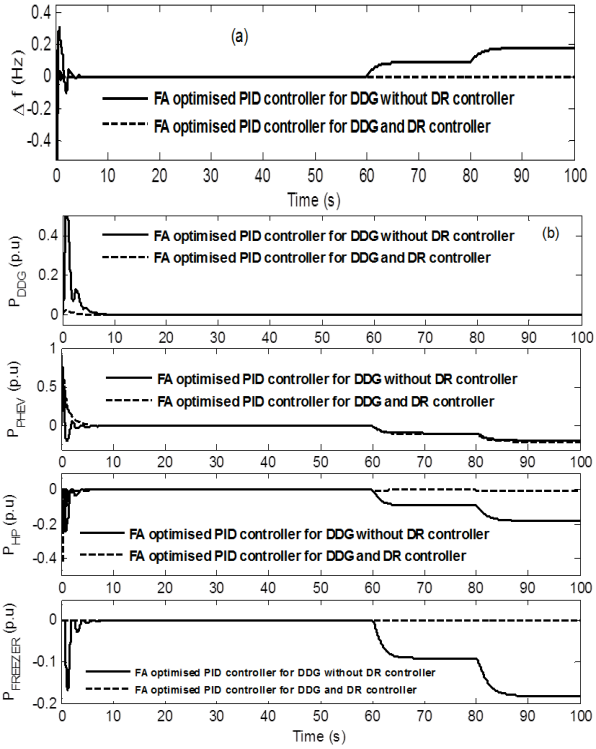

Fig. 11. (a) Frequency deviation (b) output power with FA optimized PID controllers for DDG with and without DR controller, case 1

In order to justify the performance of then DR controllers employed with the controllable loads, a comparative analysis has been conducted considering operating conditions mentioned in case 1. In this case, microgrid with out any DR controller for the controllable loads (only PID controller for the DDG) vis-à-vis microgrid with DR controllers for the controllable loads (with PID controller for the DDG) have been simulated. Frequency deviation as shown in Fig. 11 (a), indicates that microgrid without DR controllers cannot maintain the frequency to minimum level as compared to the microgrid with DR controller.

It may be noted that in this FA optimised PID controller has been used here since its performance is the best amongst all other controllers. Fig. 11 (b) represents the power absorbed or supplied by the diffrent units.

6.2 Step decrease in wind and PV power with constant demand condition: Case 2

In this study, the system is tested in the presence of wind and PV output fluctuations with constant critical load demand as shown in Fig. 12. In this case, during the period 0<t<100 s, the load demand is constant 0.5 p.u. To investigate the system response due to the step change in input power, at t=60s wind power has dropped to 0.1 p.u from its initial value 0.3 p.u, however at t=80 s, solar PV power has decreased to 50% from its initial value 0.2 p.u.

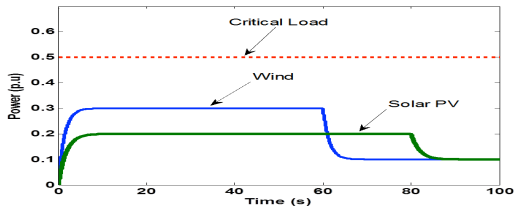

Fig. 12. Output power of P_{WTG}, P_{PV} and load model, case 2

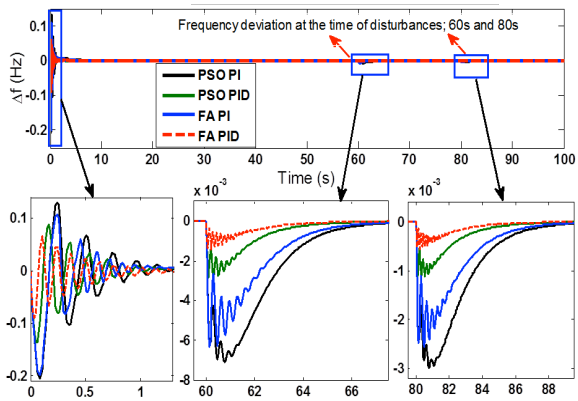

Fig. 13. Frequency deviation Δf observed with PSO and FA optimized PI and PID controllers, case 2

During 0<t<60 s, the power generated by solar PV and wind turbine generator is same as critical load demand, so no power generation from DDG and PHEV hence non- critical load (P_{NCL}) i.e., HP and FREEZER will on. However, during 60<t<100 s, the power generated from wind and solar PV system is not sufficient to supply the critical load demand; thus DDG and PHEV come in the scenario to provide the deficit power. Fig. 13 represents the comparative performance of transient response of frequency deviation for the present system using PSO and FA optimized PI/PID controller parameters.

However, the output power of DDG, PHEV, HP and FREEZER are shown in Fig. 14. Under the variation of generation and load demand, the PI and PID controllers' parameters are optimized and their values are presented in Table 3. and Table 4. respectively.

Table 3. Gains of PSO and FA opitimized PI controller.

Gains	Case 1		Case 2	
	PSO	FA	PSO	FA
K_{PDDG}	-1.4	-0.2	-0.5	-5
K_{IDDG}	-8.3	-10.05	-10.7	-15.74
K_{PPHEV}	4.62	9	10	8.99

K_{IPHEV}	1	6.26	0.23	.01469
K_{PHP}	5.1	5.57	31.42	9.12
K_{IHP}	5	8.047	0.4	0.0178
$K_{PFREEZER}$	0.01	0.0104	2	0.93
$K_{IFREEZER}$	0.1	0.3872	1.7	10
Gains	**Case 3**		**Case 4**	
K_{PDDG}	-1.2	-0.01	-1.4	-0.01
K_{IDDG}	-12.7	-20.05	-15.7	-12.16
K_{PPHEV}	12	20	10	20
K_{IPHEV}	0.3	1	0.1	0.1
K_{PHP}	5	7	5	2.8988
K_{IHP}	3	5.213	3	7.3435
$K_{PFREEZER}$	1.3	9.139	1.94	5.5562
$K_{IFREEZER}$	0.3	1.87	0.8	5.7508

Table 4. Gains of PSO and FA opitimized PID controller.

	Case 1		**Case 2**	
Gains	**PSO**	**FA**	**PSO**	**FA**
K_{PDDG}	-0.5	-0.1	-0.5	-6
K_{IDDG}	-10	-5	-20	-12.396
K_{DDDG}	-0.1	-0.0313	-0.1	0.001
K_{PPHEV}	18	15	20	40
K_{IPHEV}	19.5	43.14	20	80
K_{DPHEV}	200.61	200.484	200	100.498
K_{PHP}	30	10.948	18	20.1073
K_{IHP}	8	7	0.001	0.0263
K_{DHP}	200.63	0.0605	200.64	1.5413
$K_{PFREEZER}$	3.4	1.0654	20.64	0.1188
$K_{IFREEZER}$	2	4.0514	0.01	0.1173
$K_{DFREEZER}$	2.2	1.5526	20	0.8671
Gains	**Case 3**		**Case 4**	
K_{PDDG}	-0.01	-0.5	-0.8	-0.1
K_{IDDG}	-20	-20.953	-20	-14
K_{DDDG}	-0.1	-0.01	-1	-0.01
K_{PPHEV}	40	100	60	85
K_{IPHEV}	40.85	80.8497	5.84	8.001
K_{DPHEV}	200	266.008	20	20.3343
K_{PHP}	1.685	1.78	4.25	4.0507
K_{IHP}	1.1945	1	0.80	2.1244
K_{DHP}	300	200	2.33	1.0640
$K_{PFREEZER}$	2	80	1	0.0213
$K_{IFREEZER}$	0.6160	8	0.1	0.0592
$K_{DFREEZER}$	153.64	200.2	1.07	0.1888

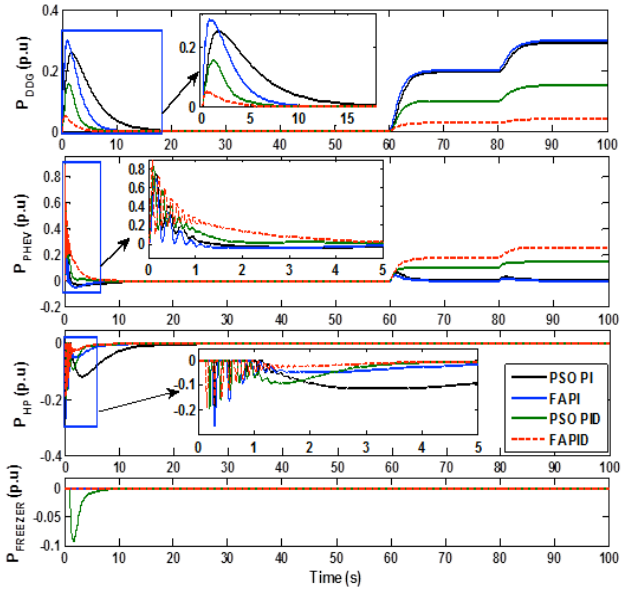

Fig. 14. Output power generation of DDG, PHEV, HP and FREEZER, case 2

The responses of frequency deviation in Fig. 13 and convergence plot in Fig. 10 clearly reveal that FA optimized controllers performed better than their PSO optimized counterparts.

6.3 Step increase in wind and PV power and step increase in demand: Case 3

In this scenario, the critical load is assumed to be 0.5 p.u during the first 60 s, and at 60<t<100 s it increase 40% (0.7 p.u) from its initial value. As it can be seen that at t= 60 s, the wind power (P_{WTG}) is increased to 0.4 p.u from its initial value of 0.3 p.u. and at t=80s, the solar PV power (P_{PV}) is increase to 0.3 p.u from its initial value of 0.2 p.u. Fig. 15 illustrated the P_{WTG}, P_{PV}, and P_{CL} respectively.

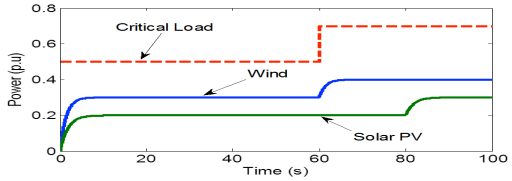

Fig. 15. Output power of P_{WTG}, P_{PV} and load model, case 3

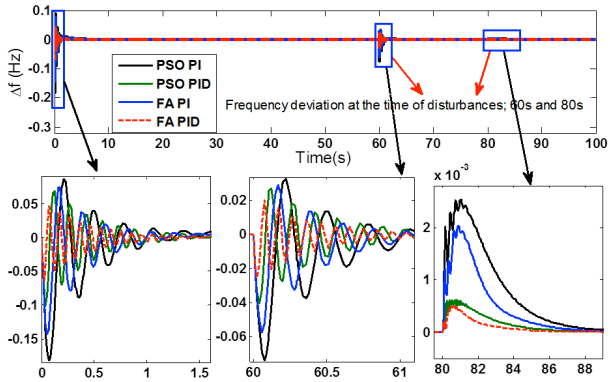

Fig. 16. Frequency deviation Δf observed with PSO and FA optimized PI and PID controllers, case 3

During the time period from 0<t<60 s, the total renewable power generation (P_S) is same as load demand, so, no need to generate power from DDG and PHEV. But during 60<t<80 s, power generated from wind and PV is not sufficient to supply the required critical load demand (P_{CL}), the diesel driven generator (DDG) and plug-in hybrid vehicles (PHEV) come into the picture and starts generating power. Hence, DSM is get activated and there is no power consumption by the HP and FREEZER. However, for the remaining time period, generated power (P_S) is same as load demand (P_{LOAD}), hence there is no power generation from DDG and PHEV.

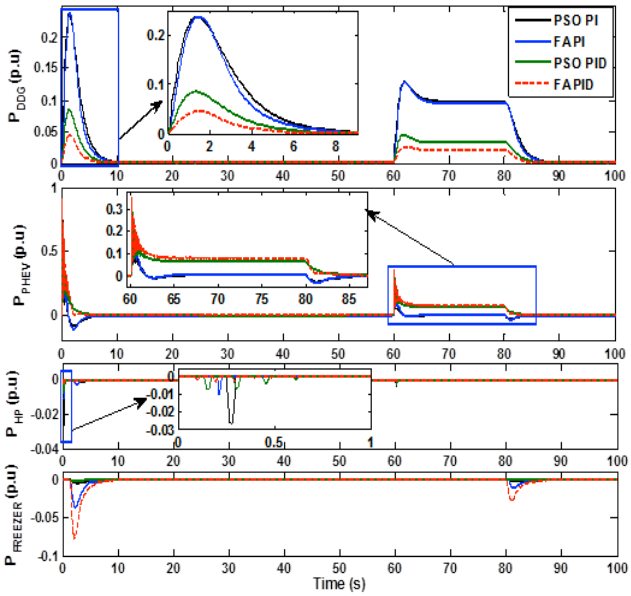

Fig. 17. Output power generation of DDG, PHEV, HP and FREEZER, case 3

Fig. 16 represents the frequency deviation of the present system using PSO and FA optimized PI/PID controller's parameters. The gains value of the PI and PID controllers parameters are presented in Table 3 and Table 4. The output power from DDG, PHEV, HP and FREEZER are shown in Fig. 17. Response of frequency deviation reveals that the FA optimized controllers perform betters than their PSO optimized counterparts.

6.4 Random variation in solar PV, wind power as well as load demand: Case 4

In this case, the dynamic performance of the present system under randomly variable characteristics of the solar PV, wind and load demand are carried out. As it can be seen that during the entire time periods the critical load, wind and solar PV power vary around the average values of 0.6 p.u, 0.3 p.u and 0.2 p.u respectively. Fig. 18 illustrate wind power (P_{WTG}), solar PV power (P_{PV}) and critical load demand (P_{CL}) under randomly varying conditions. During the time period from 0<t<100 s, the total average power generation from the intermittent energy sources is not equal to average load demand. Hence DSM get activated to control the system frequency within its limit.

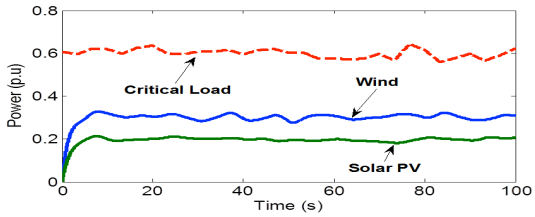

Fig. 18. Output power of P_{WTG}, P_{PV} and load model, case 4

Fig. 19 represents the frequency fluctuation when employing with PSO and FA optimized PI and PID controllers. In order to eliminate the difference between active power generation and load demand under these conditions, the output power of the DDG, PHEV, HP and FREEZER are controlled to appropriate values using controllers. The gains of the controllers (PI/PID) are obtained using PSO and FA and are presented in Table 3. and Table 4.

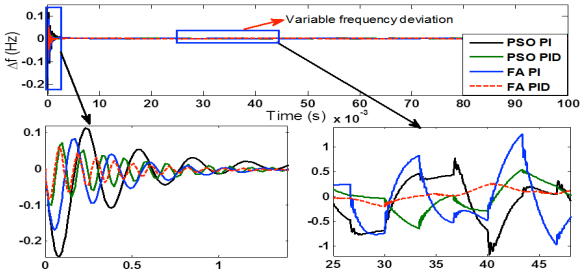

Fig. 19. Frequency deviation Δf observed with PSO and FA optimized PI and PID controller, case

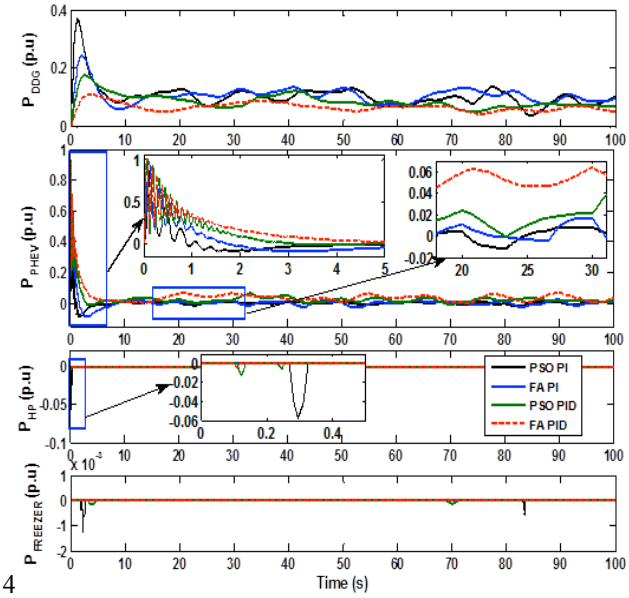

4

Fig. 20. Output power generation of DDG, PHEV, HP and FREEZER, case 4

The output power from DDG, PHEV, HP and FREEZER are shown in Fig. 20. The convergence plots of the objective function vs iteration could not be provided to limit the paper size. However, the objective function vs iteration indicate that FA optimized controllers perform better than the PSO optimised counterparts. Response of frequency deviation also reveals that the FA optimized controllers perform better than their PSO optimized counterparts. Table 5. presents the peak values of the frequency deviation for various operating condition of the systems.

Table 5. Maximum frequency deviation (Δf in Hz)

Case	Case 1		Case 2	
Time (s)	t=60s	t=80s	t=60s	t=80s
Δf	Over shoot	Over shoot	Under shoot	Under shoot
PSO PI	0.00232	0.002239	- .006323	- .002358
FA PI	0.00184	0.001469	- .005498	- 0.00212
PSO PID	0.00112	0.001118	- 0.00364	- .000887
FA PID	**0.000821**	**0.000492**	**- 0.00135**	**- .000532**
Case	**Case 3**		**Case 4**	
Time (s)	t=60s	t=80s	Random	
Δf	Under shoot	Over shoot	Overshoot/ Undershoot	
PSO PI	-0.05514	0.00133	- 0.005125	
FA PI	-0.05081	0.001061	0.0001899	
PSO PID	-0.04048	0.000687	0.0001731	
FA PID	**-0.02573**	**0.000201**	**0.000085**	

7. Conclusion

DSM, particularly direct load control is an effective control strategy in a microgrid, especially for power fluctuation caused by renewable energy resources. The present work investigates robust frequency control strategy of a solar PV, wind, DDG, PHEV, HP and FREEZER based microgrid in absence of battery energy storage using direct load control strategy along with generation control. Depending on the difference between generation and demand, DDG and PHEV along with non-critical loads are controlled using controllers (PI/PID) to deliver the steady-state frequency regulation in the system. Parameters of the PI and PID controllers are optimized by using PSO and FA algorithm techniques under different generation and load demand condition. Simulation results demonstrate the effectiveness of proposed demand side management (DSM) strategy. Though there are variations of P_{WTG}, P_{PV}, and P_{CL}; the power generation from DDG, PHEV and non-critical loads can effectively controlled using DSM strategy in absence of battery bank storage. Furthermore, the comparative performance of robustness of FA optimized controllers in comparison to PSO optimized controllers reveals that FA optimized controllers is superior. The convergence plots of FA optimized controller are much better than PSO optimized controllers. So, it can be conclude that the performance of the proposed control scheme is excellent in regulating the frequency in all the cases.

Appendix

K_{WTG} = 1, T_{WTG} = 1.5 s, K_{PV} = 1, T_{PV} = 1.8 s, K_G = 1, T_G = 0.1 s, K_{DDG} = 1, T_{DDG} = 0.4s, K_{PHEV} = -1, T_{PHEV} = 0.2 s, K_{HP} = -1, T_{HP} = 0.1 s, $K_{FREEZER}$ = -1, $T_{FREEZER}$ = 0.2456 s, D= 0.2 (pu/Hz), R = 3 (Hz/pu), M = 0.012 (pu s).

Acknowledgements

The authors would like to thanks NIT Silchar for giving the necessary supports to carry this work

References

[1] B. Christopher "Dynamic Demand Balancing Using DSM Techniques in a Grid-Connected Hybrid System", *International Journal of Renewable Energy Research (IJRER)* vol. 4, no. 4, pp. 1031-1041, 2014. (Article)

[2] J. Yang, Z. Zeng, Y. Tang, J. Yan, H. He, & Y. Wu, "Load frequency control in isolated micro-grids with electrical vehicles based on multivariable generalized predictive theory", *Energies* vol. 8, no. 3, pp. 2145-2164, 2015. (Article)

[3] U. Markovic, "Fast Demand Response with Cooling Devices", 2014.

[4] A. H. Mohsenian-Rad, V. W. Wong, J. Jatskevich, R. Schober, and A. Leon-Garcia, "Autonomous demand-side management based on game-theoretic energy consumption scheduling for the future smart grid", *IEEE Trans. on Smart Grid* vol. 1, no. 3, pp. 320-331, 2010. (Article)

[5] R. Ali, T. H. Mohamed, Y. S. Qudaih, and Y. Mitani, "A new load frequency control approach in an isolated small power systems using coefficient diagram method", *International Journal of Electrical Power & Energy Systems* vol. 56, pp. 110-116, 2014. (Article)

[6] M. S. Bisht, "Fuzzy based intelligent frequency control strategy in standalone hybrid ac microgrid", *Proceeding IEEE Conference*, *In Control Applications (CCA),* pp. 873-878, 8-10 October 2014. (Conference Paper)

[7] H. Bevrani, F. Habibi, P. Babahajyani, M. Watanabe, and Y. Mitani, "Intelligent frequency control in an AC microgrid: Online PSO-based fuzzy tuning approach", *IEEE Trans. on Smart Grid* vol. 3, no. 4, pp. 1935-1944, 2012. (Article)

[8] D. C. Das, N. Sinha, and A. K. Roy, "Automatic Generation Control of an Organic Rankine Cycle Solar–Thermal/Wind–Diesel Hybrid Energy System", *Energy Technology* vol. 2, no. 8, pp. 721-731, 2014. (Article)

[9] D. J Lee and L. Wang, "Small-signal stability analysis of an autonomous hybrid renewable energy power generation/energy storage system part I: Time-domain simulations", *IEEE Trans. on Energy Conversion* vol. 23, no. 1, pp. 311-320, 2008. (Article)

[10] C. Wang, and M.H. Nehrir, "Power management of a stand-alone wind/photovoltaic/fuel cell energy

system", *IEEE Trans. on energy conversion* vol. 23, no. 3, pp. 957-967, 2008. (Article)

[11] H.R. Kermani, M.V. Dahraie, and H.R. Najafi, "Demand response strategy for frequency regulation in a microgrid without storage requirement", *24th Iranian Conference on Electrical Engineering (ICEE),* pp. 921-926, 10-12 May 2016. (Conference Paper)

[12] M. R. Aghamohammadi, & H. Abdolahinia, "A new approach for optimal sizing of battery energy storage system for primary frequency control of islanded microgrid", *International Journal of Electrical Power & Energy Systems* vol. 54, pp. 325-333, 2014. (Article)

[13] Z. Xu, X. Guan, Q. S. Jia, J. Wu, D. Wang, & S. Chen, "Performance analysis and comparison on energy storage devices for smart building energy management", *IEEE Trans. on Smart Grid* vol. 3, no. 4, pp. 2136-2147, 2012. (Article)

[14] Y. Ozturk, D. Senthilkumar, S. Kumar, and G. Lee, "An intelligent home energy management system to improve demand response", *IEEE Trans. on Smart Grid* vol. 4, no. 2, pp. 694-701, 2013. (Article)

[15] Y.Q. Bao, Y. Li, Y.Y. Hong, and B. Wang, "Design of a hybrid hierarchical demand response control scheme for the frequency control", *IET Generation, Transmission & Distribution* vol. 9, no. 15, pp. 2303-2310, 2015. (Article)

[16] P. C Sekhar., and S. Mishra, "Storage free smart energy management for frequency control in a diesel-PV-fuel cell-based hybrid AC microgrid", *IEEE Trans. on neural networks and learning systems* vol. 27, no. 8, pp. 1657-1671, 2016. (Article)

[17] J. Wang, H. Zhang, & Y. Zhou, "Intelligent under frequency and under voltage load shedding method based on the active participation of smart appliances", *IEEE Trans. on Smart Grid* vol. 8, no. 1, pp. 353-361, 2017. (Article)

[18] Cheng, Ming, and Ying Zhu, "The state of the art of wind energy conversion systems and technologies: A review", *Energy Conversion and Management* vol. 88, pp. 332-347, 2014. (Article)

[19] I. Hussain, S. Ranjan, D.C. Das, and N. Sinha, "Performance Analysis of Flower Pollination Algorithm Optimized PID Controller for Wind-PV-SMES-BESS-Diesel Autonomous Hybrid Power System", *International Journal of Renewable Energy Research (IJRER)*, vol. 7, no. 2, pp.643-651, 2017. (Article)

[20] R. Bouchebbat, and S. Gherbi, "A Novel Optimal Control and Management Strategy of Stand-Alone Hybrid PV/Wind/Diesel Power System", *Journal of Control, Automation and Electrical Systems* vol. 28, no. 2, pp. 284-296, 2017. (Article)

[21] J. Cao, and A. Emadi, "A new battery/ultracapacitor hybrid energy storage system for electric, hybrid, and plug-in hybrid electric vehicles", *IEEE Trans on power electronics* vol. 27, no. 1, pp. 122-132, 2012. (Article)

[22] S. Kawachi, J. Baba, H. Hagiwara, E. Shimoda, S. Numata, E. Masada, and T. Nitta, "Energy capacity reduction of energy storage system in microgrid by use of heat pump: characteristic study by use of actual machine", *14th International Power Electronics and Motion Control Conference (EPE/PEMC),* Macedonia, pp. T11-52, 6-8 September 2010. (Conference Paper)

[23] Y. Qi, H. Jia, and Y. Mu, "Dynamic frequency control of autonomous microgrid based on family-friendly controllable loads", *Innovative Smart Grid Technologies (ISGT), 2013 IEEE PES*, Washington, pp. 1-6, 24-27 February 2013. (Conference Paper)

[24] S. Kumar, and A.J. Veronica, "Load Frequency Controller Design for Microgrid Using Internal Model Approach", *International Journal of Renewable Energy Research (IJRER)*, vol. 7, no. 2, pp.778-786, 2017. (Article)

[25] Y. Del Valle, G. K. Venayagamoorthy, S. Mohagheghi, J.-C. Hernandez, and R. G. Harley, "Particle swarm optimization: basic concepts, variants and applications in power systems", *IEEE Trans. on evolutionary computation* vol. 12, no. 2, pp. 171-195, 2008. (Article)

[26] S.K. Meena, and S. Chanana, "Load Frequency Control of multi area system using Hybrid Particle Swarm Optimization", *2nd International Conference on Recent Advances in Engineering & Computational Sciences (RAECS),* Chandigarh, 21-22 December, 2015. (Conference Paper)

[27] A.H. Gandomi, X.S. Yang, S. Talatahari, A.H. Alavi, "Firefly algorithm with chaos", *Communications in Nonlinear Science and Numerical Simulation* vol. 18, no. 1, pp. 89-98, 2013. (Article)

[28] X.S. Yang "Firefly algorithm for multimodal optimization, stochastic algorithms foundations and applications", *Lecture notes in Computer Sciences,* vol. 5792. p. 169–178, SAGA 2009. (Book Series)

[29] L.C. Saikia, S. K. Sahu, "Automatic generation control of a combined cycle gas turbine plant with classical controllers using firefly algorithm", *International Journal of Electrical Power & Energy Systems* vol. 53, pp. 27-33, 2013. (Article).